Journal of Physics: Conference Series **653** (2015) 012001 doi:10.1088/1742-6596/653/1/012001

The behavior of tantalum under ultrashort loads induced by femtosecond laser

S I Ashitkov, P S Komarov, E V Struleva, M B Agranat, G I Kanel and K V Khishchenko

Joint Institute for High Temperatures of the Russian Academy of Sciences, Izhorskaya 13 Bldg 2, Moscow 125412, Russia

E-mail: ashitkov11@yandex.ru

Abstract. We studied the shock-wave and ablation phenomena in tantalum films of submicron thicknesses irradiated by femtosecond laser pulses. The single-shot spectral interferometry was used for continuous diagnostics of movement in a picosecond range both the frontal and rear surfaces of a sample. Measured displacement histories were converted into surface velocity histories. As a result, the new data on shear and tensile strength have been obtained for solid and molten tantalum at strain rate $\sim 10^9$ s^{-1}.

1. Introduction

It is known that the resistance of materials to deformation and fracture increases with the increasing of a strain rate. There are the ultimate value of tensile strength, the so-called "ideal" strength that is equal to the negative pressure at which the bulk modulus turns to zero. The results of the first experiments [1–5] of shock-wave phenomena induced under nonequilibrium heating [6] by femtosecond laser pulses of thin film metallic samples convincingly demonstrated that shear and tensile stresses close to their extremely possible "ideal" values can be achieved under these conditions. Such investigations provide the data for the development of the physical theory of strength and plasticity of solids, construction of models of interaction and forecasting of the behavior of materials in a wide range of the loads, for testing of the hydrodynamic and atomistic simulations [7, 8].

In this article, the results of experimental study of shear and tensile strength of tantalum are presented. Here we continue our previous investigation of femtosecond laser driven high-rate deformations in metals in a picosecond time range using chirped pulse interferometry [2–5, 9, 10]. This technique allows for continuously recording the temporal dependence of the spatially nonuniform surface motion in a single experiment with picosecond time resolution. In experiments, we measured time and spatial resolved displacement of both the frontal and rear surfaces of tantalum films. The application of Fourier processing of interference patterns ensures the measurement of the displacement of the target surface with an accuracy of several nanometers. Unlike multipulse femtosecond interferometric microscopy [1], this single shot technique provides a much higher reliability of the measurements.

2. Experiment and discussion

The CPA Ti:sapphire femtosecond laser system was used for generation and diagnostics of the shock-wave phenomena. After the regenerative amplifier, a chirped pulse of 300 ps duration was split into two parts. A weaker frequency modulated (chirped) probe pulse at the central wavelength $\lambda_0 = 795$ nm with bandwidth FWHM $\Delta\lambda = 23$ nm was used for diagnostics of target's movement. A powerful part with the energy up to 1 mJ was compressed to a pulse of 500 fs duration. The tested samples were the tantalum film of 510 and 820 nm in thicknesses deposited by magnetron sputtering on borosilicate glass substrates of 150 μm in thickness.

In the first series of experiments the pump beam was focused on a glass-metal interface through the transparent substrate, and the probe beam detected the dynamics of shock breakout on a free rear surface of the film (figure 1).

Pump pulse was focused by the lens with $f = 30$ cm onto a surface of the film in a Gaussian spot with a diameter of 48 μm at the e^{-1} level. The diagnostic part of the setup was a Michelson interferometer, where one of the mirrors was the rear surface of the sample. An objective with NA = 0.2 was used to transfer the image of rear surface to the input slit of the imaging diffraction spectrometer Acton 2300i. The values of temporal and longitudinal spatial resolution were 1 ps and 2 μm respectively. The interferometer was adjusted in such a way that the interference fringes were perpendicular to the input slit of spectrometer. The interference pattern at the output of the spectrometer was recorded by a CCD-camera. The wavelength in a recorded spectrum was juxtaposed to time, whereas the other axis (along the slit) corresponded to spatial coordinate on a target.

In each measurement three interferograms were recorded: before, during, and after the shock wave breakout. The applied algorithm of Fourier processing of interference patterns [5, 9] provides accuracy of a phase shift measurement of about ≈ 0.01 rad, which corresponds to 1–2 nm of the error in a surface displacement.

In the second series of experiments we investigated a process of thermomechanical ablation to obtain the data on tensile strength of tantalum in a liquid state. In this case the experimental scheme was modified. The pump beam was focused on the surface of metal film at an angle of incidence of 60°, and probe beam monitored the expansion dynamics of the heated frontal surface [10].

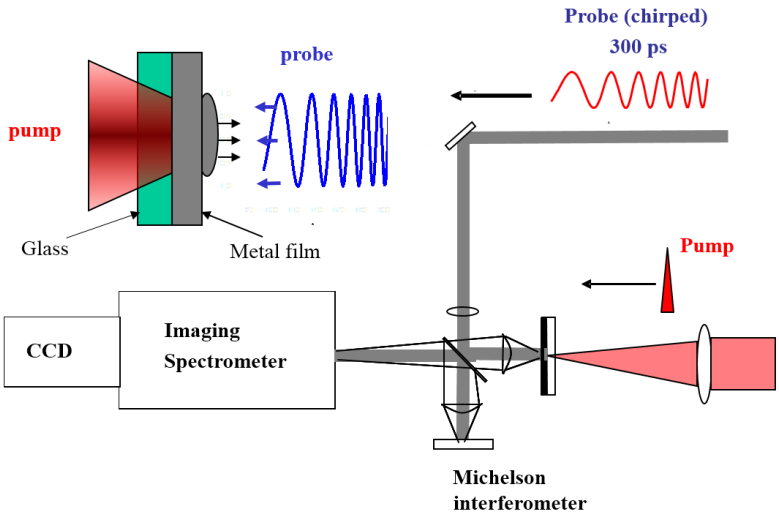

Figure 1. Scheme of the shock-wave experiment.

Figure 2 summarizes the displacement histories obtained from the central area of the breakout profile for several laser shots. The results demonstrate high reproducibility of the measurements in the initial stage of the surface motion. A small relative shift of the profiles in time is probably due to small variation of the sample thickness. A significant discrepancy of the histories at delays more than 30–50 ps with respect to the beginning of motion is associated with the process of spall fracture.

Figure 3 shows the free rear surface displacement history $z(t)$ measured for central part of the focal spot. The free surface velocity profiles $u_{\rm fs}(t)$ were evaluated by differentiating the measured $z(t)$ dependence with the subsequent iteration procedure, as a result of which the integral $u_{\rm fs}(t)$ is the best fit of the measured displacement history (figure 3). The obtained velocity histories for the free rear (blue line) and frontal (green line) surfaces are presented. The last one was measured in the vicinity of ablation threshold.

The averaged speed of shock wave in the 510–820 nm section, determined from the measured time interval between the shock arrivals, has been found equal to $U_s = 5.0 \pm 0.3$ km/s. The averaged maximal value of free surface velocity $u_{\rm fs}^{\rm max}$ decreases from 1.0 to 0.6 km/s at this propagation distance. A comparison of the shock wave speed and particle velocity $u_p = u_{\rm fs}^{\rm max}/2$ shows that the measured value U_s is much higher than Hugoniot $U_s = c_b + bu_p$ (where $c_b = 3.4$ km/s; $b = 1.2$) obtained in plate impact experiments [11]. High propagation speed and absence of the wave splitting into elastic-plastic two-wave configuration point out that plastic deformation were not developed in picosecond time domain and the detected shock wave is purely elastic. This assumption is supported by its small rise time of order 1–2 ps that indicated an insignificant contribution of dissipative processes.

Using the results of measurement and the value $c_l = 4.14$ km/s for the longitudinal speed of sound in tantalum at normal pressure, the Hugoniot of elastic compression of tantalum can be estimated as $U_s = 4.14 + 2.0u_p$.

Figure 4 presents results of measurements on the stress-strain plane. In the shot shown in figure 4, the deviatoric stress $\sigma_x - p$ reached 18.7 GPa that corresponds to maximum shear

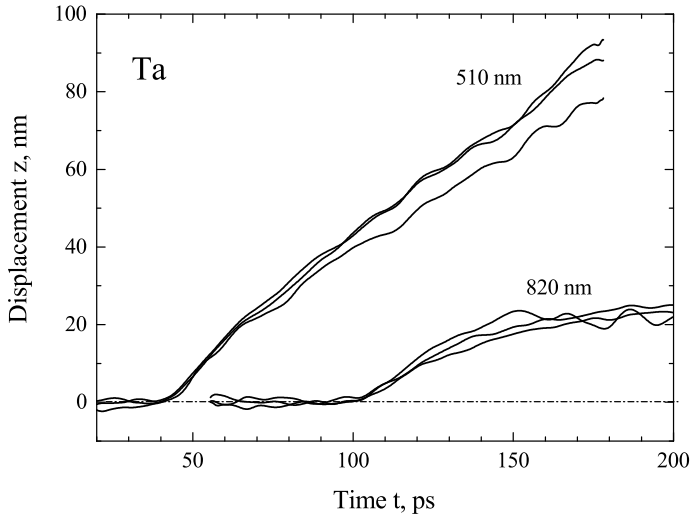

Figure 2. The arrays of the free surface displacement profiles of shocked tantalum samples of 510 and 820 nm. For all figures zero time moment was chosen arbitrarily.

stress at uniaxial compression [12] $\tau = (3/4)(\sigma_x - p) = 14$ GPa. Figure 5 shows the measured parameters of the elastic shock wave in tantalum in comparison with the data from plate impact experiments [13] on the dependence of the Hugoniot elastic limit σ_{HEL} on the distance passed by the wave.

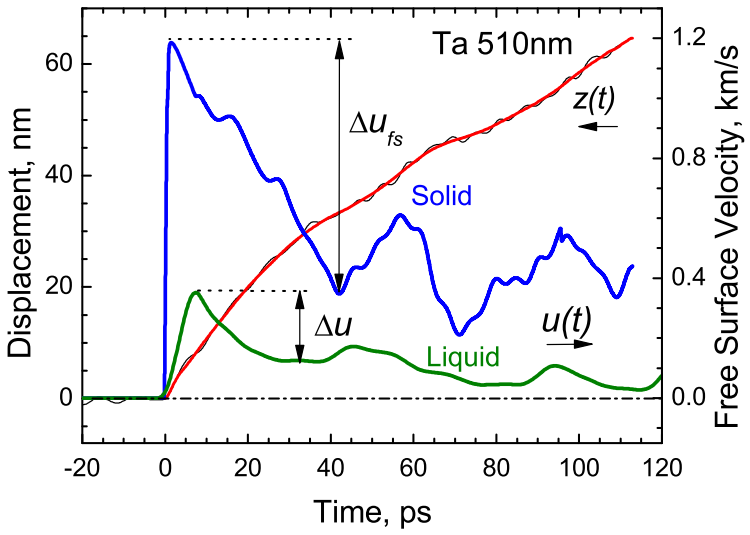

Figure 3. The example of processing of the displacement profile for tantalum samples of 510 nm in thickness; thin black line shows the measured $z(t)$ profile; the solid lines show the results of the iteration procedure.

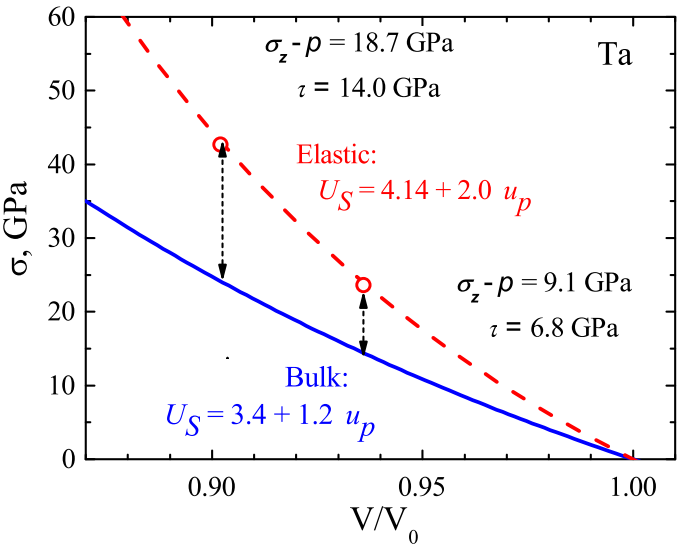

Figure 4. Measured states in elastic shock waves (points) in comparison with Hugoniot of solid tantalum.

The reflection of the compression pulse from the free surface of the sample results in the appearance of tensile stresses inside the sample. The magnitude of stresses increases as the reflected wave propagates from the surface into the bulk of the sample. When the tensile stresses exceed the strength of the material σ_{spall}, a fracture occurs [14, 15]. The relaxation of stresses leads to the formation of a secondary compression wave, the so-called spall pulse. Reaching the free surface, this pulse again increases the velocity of the surface.

The spall strength was determined using measured velocity pullback (see figure 3) for triangular load profile by expression [15]

$$\sigma_{\text{spall}} = \rho c_l \Delta u_{\text{fs}} \frac{1}{1 + c_l/c_b}.$$

Here $\rho = 16.6$ g/cm^3, $c_l = 4.14$ km/s, $c_b = 3.4$ km/s are density, longitudinal and bulk sound speeds respectively. For maximal measured value $\Delta u_{\text{fs}} = 0.86$ km/s the estimated value σ_{spall} for tantalum reached 26.7 GPa at the strain rate of $V/V_0 \approx 5 \times 10^9$ s^{-1}.

The tensile strength value of liquid tantalum σ_{liq} can be roughly estimated using the acoustic relation [16]:

$$\sigma_{\text{liq}} = \rho_{\text{liq}} c_{\text{liq}} \Delta u/2.$$

For the experimentally determined value $\Delta u = 0.22$ km/s (see figure 3) and taking for liquid tantalum density and sound velocity $\rho_{\text{liq}} \approx 13.8$ g/cm^3, $c_{\text{liq}} \approx 2.9$ km/s according to an equation of state [17], we obtain the estimation $\sigma_{\text{liq}} \approx 4.4$ GPa at the strain rate of $V/V_0 \approx 1.5 \times 10^9$ c^{-1}.

The value of σ_{liq} was determined in vicinity of ablation threshold F_a. Let us estimate the temperature T of molten tantalum near F_a. The measured values of ablation threshold and pump reflectivity for the considered experimental conditions ($\lambda = 800$ nm, $\theta = 60°$, p-polarization) were $F_a \approx 0.28$ J/cm^2 and $R \approx 0.4$.

Fast laser heating rises pressure in the heated layer d_T and therefore produces acoustic wave. In case of thin samples the duration of propagating shock wave τ_s correlates with d_T [18]. Taking $U_s \approx 4$ km/s and $\tau_s \approx 25$ ps (duration of u_{fs} FWHM, figure 3) we obtain the rough estimate of

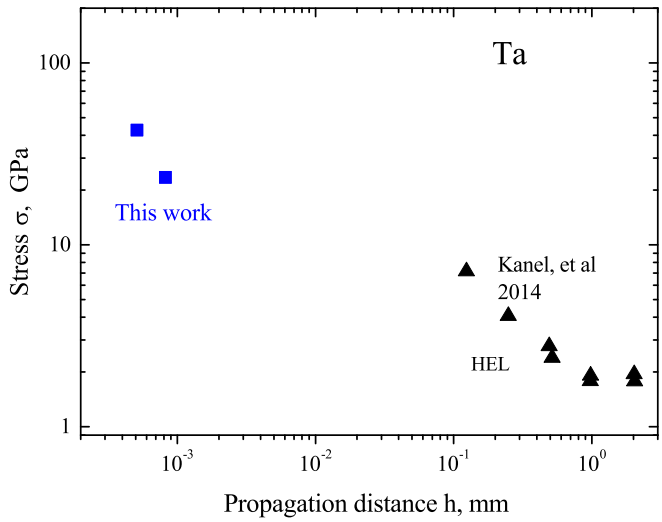

Figure 5. Decay of the elastic shock wave in tantalum.

$d_T \approx U_s\tau_s \approx 100$ nm. Definition of temperature follows from the expression

$$(1-R)F_a/d_T = C\rho(T-T_0) - \Delta H_m,$$

where specific heat capacity is $C = 0.151$ J/g/K; heat of melting $\Delta H_m = 35$ kJ/mol; $T_0 = 300$ K. The estimated value of temperature $T \approx 5$ kK of surface layer is higher than melting temperature of tantalum $T_m \approx 3288$ K .

Figure 6 shows the tensile strength of solid and liquid tantalum as a function of the strain rate obtained in this work in comparison with the data of earlier experiments and calculations (see [19, 20] and references therein). The extrapolation to the higher strain rates predicts the achievement of the "ideal" tensile strength of solid tantalum at the rate of about $V/V_0 \sim 10^{11}$ s^{-1}.

3. Summary

Thus in this work we have implemented single shot chirped pulse interferometry for measuring both the ablation dynamics and propagation of ultra short shock waves in submicron tantalum films irradiated by femtosecond laser pulses. The relation between shock wave velocity and the particle velocity indicates that shock compression is elastic up to 42.7 GPa in this range. The shear stresses behind the shock in this case reach 14 GPa. The tensile strength of 4.4 and 27 GPa of liquid and solid tantalum respectively has been measured at extremely high strain rates of (1–5) $\times 10^9$ s^{-1}. The obtained value of tensile strength of solid tantalum is closed to the theoretical ultimate value.

Acknowledgments

This work was financially supported by grants of the Russian Foundation for Basic Research (No. 13-02-91057 and 14-08-00967) and the President of the Russian Federation (No. NSh-

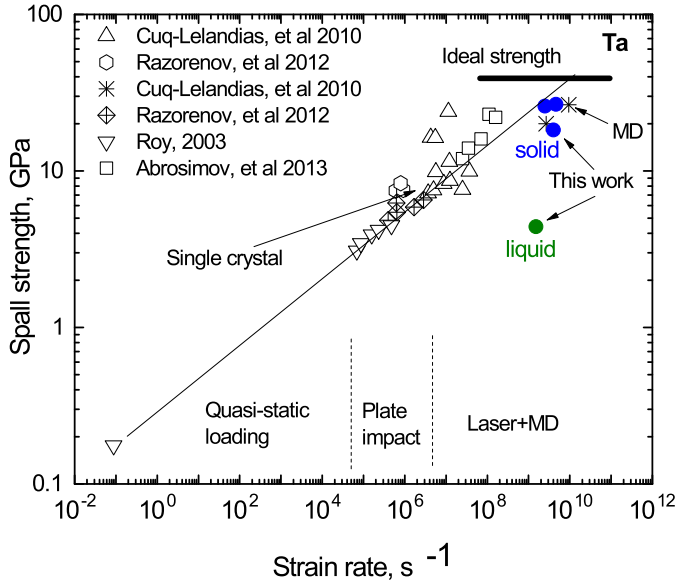

Figure 6. Measured spall strength of tantalum in comparison with data of previous experiments and results of molecular dynamics simulations.

4082.2014.1 and NSh-6614.2014.2), as well as the programs of the Presidium RAS (No. 13P "Thermal physics of high energy densities").

References

[1] Ashitkov S I, Agranat M B, Kanel G I and Fortov V E 2010 *JETP Lett.* **92** 516
[2] Whitley V H, McGrane S D, Eakins D E, Bolme C A, Moore D S and Bingert J F 2011 *J. Appl. Phys.* **109** 013505
[3] Crowhurst J C, Armstrong M R, Knight K B, Zaug J M and Behymer J F 2011 *Phys. Rev. Lett.* **107** 144302
[4] Ashitkov S I, Komarov P S, Agranat M B, Kanel G I and Fortov V E 2013 *JETP Lett.* **98** 384
[5] Ashitkov S I, Komarov P S, Struleva E V, Agranat M B and Kanel G I 2015 *JETP Lett.* **101** 276
[6] Agranat M B, Ashitkov S I, Ovchinnikov A V, Sitnikov D S, Yurkevich A A, Chefonov O V, Perel'man L T, Anisimov S I and Fortov V E 2015 *JETP Lett.* **101** 598
[7] Andreev N E, Povarnitsyn M E, Veysman M E, Faenov A Ya, Levashov P R, Khishchenko K V, Pikuz T A, Magunov A I, Rosmej O N, Blazevic A, Pelka A, Schaumann G, Schollmeier M and Roth M 2015 *Laser Part. Beams* **33** 541
[8] Povarnitsyn M E, Fokin V B and Levashov P R 2015 *Appl. Surf. Sci.* **357** 1150
[9] Geindre J P, Audebert P, Rebibo S, and Gauthier J C 2001 *Opt. Lett.* **26** 1612
[10] Ashitkov S I, Komarov P S, Ovchinnikov A V, Struleva E V, Zhakhovskii V V, Inogamov N A and Agranat M B 2014 *Quantum Electron.* **44** 535
[11] Fortov V E, Altshuler V L, Trunin R F and Funtikov A I 2000 *Shock Waves and Extreme States of Matter* (Moscow: Nauka)
[12] Zeldovich Ya B and Raizer Yu P 1967 *Physics of Shock Waves and High Temperature Hydrodynamic Phenomena* (New York: Academic)
[13] Zaretsky E B and Kanel G I 2014 *J. Appl. Phys.* **115** 243502
[14] Kanel G I, Razorenov S V and Fortov V E 2004 *Shock-Wave Phenomena and the Properties of Condensed Matter* (New York: Springer)
[15] Kanel G I 2010 *Int. J. Fract.* **163** 173
[16] Kanel G I, Savinykh A S, Garkushin G V and Razorenov S V 2015 *JETP Lett.* **102**(8)
[17] Fortov V E, Khishchenko K V, Levashov P R and Lomonosov I V 1998 *Nucl. Instr. Meth. Phys. Res. A* **415** 604
[18] Inogamov N A, Ashitkov S A, Zhakhovsky V V, Shepelev V V, Khokhlov V A, Komarov P S, Agranat M B, Anisimov S I and Fortov V E 2010 *Appl. Phys. A* **101** 1
[19] Razorenov S V, Kanel G I, Garkushin G V and Ignatova O N 2012 *Phys. Solid State* **54** 79
[20] Abrosimov S A, Bazhulin A P, Voronov V V, Geras'kin A A, Krasyuk I K, Pashinin P P, Semenov A Yu, Stuchebryukhov I A, Khishchenko K V and Fortov V E 2013 *Quantum Electron.* **43** 246